AGU PUBLICATIONS

JGR

Journal of Geophysical Research: Atmospheres

RESEARCH ARTICLE
10.1002/2017JD027380

Key Points:
- The amount effect in the Galápagos is manifested on daily and monthly time scales
- Rare, low $\delta^{18}O$ rainfall values associated with deep convection during very strong El Niño events
- The 2015/2016 El Niño did not produce large precipitation or $\delta^{18}O$ anomalies in the Galápagos

Supporting Information:
- Data Set S1
- Supporting information S1

Correspondence to:
J. L. Conroy,
jconro@illinois.edu

Citation:
Martin, N. J., Conroy, J. L., Noone, D., Cobb, K. M., Konecky, B. L., & Rea, S. (2018). Seasonal and ENSO influences on the stable isotopic composition of Galápagos precipitation. *Journal of Geophysical Research: Atmospheres*, *123*, 261–275. https://doi.org/10.1002/2017JD027380

Received 29 JUN 2017
Accepted 12 DEC 2017
Accepted article online 18 DEC 2017
Published online 13 JAN 2018

Seasonal and ENSO Influences on the Stable Isotopic Composition of Galápagos Precipitation

N. J. Martin[1], J. L. Conroy[1,2], D. Noone[3], K. M. Cobb[4], B. L. Konecky[5], and S. Rea[6]

[1]Department of Geology, University of Illinois at Urbana-Champaign, Urbana, IL, USA, [2]Department of Plant Biology, University of Illinois at Urbana-Champaign, Urbana, IL, USA, [3]College of Earth, Ocean, and Atmospheric Sciences, Oregon State University, Corvallis, OR, USA, [4]School of Earth and Atmospheric Sciences, Georgia Institute of Technology, Atlanta, GA, USA, [5]Cooperative Institute for Research in Environmental Sciences, University of Colorado Boulder, Boulder, CO, USA, [6]Charles Darwin Research Station, Santa Cruz Island, Galápagos, Ecuador

Abstract The origin of stable isotopic variability in precipitation over time and space is critical to the interpretation of stable isotope-based paleoclimate proxies. In the eastern equatorial Pacific, modern stable isotope measurements in precipitation ($\delta^{18}O_p$ and δD_p) are sparse and largely unevaluated in the literature, although insights from such analyses would benefit the interpretations of several regional isotope-based paleoclimate records. Here we present a new 3.5 year record of daily-resolved $\delta^{18}O_p$ and δD_p from Santa Cruz, Galápagos. With a prior 13 year record of monthly $\delta^{18}O_p$ and δD_p from the island, these new data reveal controls on the stable isotopic composition of regional precipitation on event to interannual time scales. Overall, we find Galápagos $\delta^{18}O_p$ is significantly correlated with precipitation amount on daily and monthly time scales. The majority of Galápagos rain events are drizzle, or garúa, derived from local marine boundary layer vapor, with corresponding high $\delta^{18}O_p$ values due to the local source and increased evaporation and equilibration of smaller drops with boundary layer vapor. On monthly time scales, only precipitation in very strong, warm season El Niño months has substantially lower $\delta^{18}O_p$ values, as the sea surface temperature threshold for deep convection (28°C) is only surpassed at these times. The 2015/2016 El Niño event did not produce strong precipitation or $\delta^{18}O_p$ anomalies due to the short period of warm SST anomalies, which did not extend into the peak of the warm season. Eastern Pacific proxy isotope records may be biased toward periods of high rainfall during strong to very strong El Niño events.

1. Introduction

The intricacy of processes regulating El Niño–Southern Oscillation (ENSO), combined with limited observations, translates into sizeable uncertainties in future climate projections (Cai et al., 2015). A more complete understanding of ENSO requires quantitative reconstructions of ocean and climate variables spanning the tropical Pacific basin across time spans that extend beyond instrumental observations. In the eastern equatorial Pacific (EEP), several studies have provided the foundation for evaluating the history of ENSO throughout the Holocene and last glacial period using $\delta^{18}O$ values from corals or mollusks (Carré et al., 2014; Dunbar et al., 1994), marine foraminiferal assemblages and $\delta^{18}O$ values (Koutavas et al., 2002; Koutavas et al., 2004; Koutavas et al., 2006; Lea et al., 2000; Loubere et al., 2003), and other lacustrine mineralogical, sedimentological, and biological analyses (Conroy et al., 2008; Conroy et al., 2009; Moy et al., 2002; Riedinger et al., 2002). More recent Galápagos lacustrine sediment records of biomarker hydrogen isotope ratios derived from aquatic algae, cyanobacteria, and dinoflagellates have provided information on the nature of past Galápagos precipitation (Atwood & Sachs, 2014; Nelson and Sachs, 2016; Sachs et al., 2009; Zhang et al., 2014). Such records are interpreted to reflect past rainfall amount partly due to the well-known manifestation of the isotopic "amount effect": the inverse correlation between precipitation amount and the ratio of heavy to light oxygen and hydrogen isotopes in tropical precipitation (Dansgaard, 1964; Rozanski et al., 1993). As increased sea surface temperature (SST) in the EEP during canonical El Niño events spurs large, positive rainfall anomalies (Johnson, 2013; Kug et al., 2009), such proxies therefore hold great promise as indicators of ENSO variability. However, the mechanisms contributing to variations in the stable isotopic composition of precipitation remain relatively unexplored in the EEP.

In this study, we assess the stable oxygen and hydrogen isotopic ratios of Galápagos precipitation, expressed in the delta notation relative to Vienna Standard Mean Ocean Water (VSMOW):

$$\delta^{18}O = \left(\frac{\frac{^{18}O}{^{16}O}\text{sample}}{\frac{^{18}O}{^{16}O}\text{standard}} - 1\right) * 1000‰ \quad (1)$$

$$\delta D = \left(\frac{\frac{^{2}H}{^{1}H}\text{sample}}{\frac{^{2}H}{^{1}H}\text{standard}} - 1\right) * 1000‰ \quad (2)$$

We investigate the relationship between precipitation $\delta^{18}O$ values (hereafter $\delta^{18}O_p$) and δD values (hereafter δD_p) and EEP climate. In particular, we focus on the expression of the isotopic amount effect. The amount effect has been attributed to a combination of regional and local atmospheric processes, and to date there appears to be no universal singular cause. Rayleigh distillation, the progressive rainout of the heaviest water molecules during the evolution of a storm, gradually decreases residual vapor and subsequent precipitation $\delta^{18}O_p$ and δD_p values as a storm progresses (Dansgaard, 1964). Evaporation of falling rain also contributes to the amount effect (Dansgaard, 1964; Gat, 1996; Stewart, 1975). When precipitation drop size and rate increase, the evaporation rate decreases, reducing diffusion of lighter isotopologues associated with the evaporation of liquid water. The isotopic amount effect is also significantly influenced by cloud convective processes, namely rain re-evaporation and recycling of water vapor via downdrafts and updrafts, and equilibration of falling rain with isotopically lighter subcloud vapor as atmospheric convection and precipitation rates strengthen (Kurita et al., 2009; Kurita, 2013; Risi et al., 2008; Yapp, 1982). Additionally, other tropical amount effect investigations attribute decreasing $\delta^{18}O_p$ with increasing rain rate to the colder temperatures of higher-elevation convective cloud systems (Permana et al., 2016; Scholl et al., 2009). Moisture source and pathway may also influence the relationship between precipitation amount and its stable isotopic value (Cobb et al., 2007; Lawrence et al., 2004). These mechanisms have been studied in detail in the western Pacific (Berkelhammer et al., 2012; Cobb et al., 2007; Conroy et al., 2016; Kurita et al., 2009; Moerman et al., 2013); however, similar investigations of processes controlling the isotopic composition of precipitation are lacking at tropical island sites in the EEP.

In this study, we present a daily-resolved record of $\delta^{18}O_p$ and δD_p from the Galápagos Islands, located in the EEP. Analysis of 3.5 years of daily-resolved rainwater samples from Santa Cruz Island allows us to explore the atmospheric processes driving stable isotopic variability in EEP precipitation on event to seasonal time scales. We also assess the relationship between ENSO and $\delta^{18}O_p$ with this new data set, which captures the 2015/2016 El Niño event. Additionally, we analyze the 1995–2008 monthly record of Santa Cruz Island $\delta^{18}O_p$ and δD_p from the International Atomic Energy Agency (IAEA)-operated Global Network of Isotopes in Precipitation (GNIP) database (IAEA/WMO, 2016; http://www.iaea.org/water), which captures strong La Niña to very strong El Niño events. This comprehensive examination of processes controlling stable isotope ratios in precipitation from the EEP provides critical empirical support for work citing the amount effect as a primary driver of isotopic variability in past precipitation. Our results also add clarity to the spatial and temporal scope of climate variability recorded in $\delta^{18}O$ and δD-based paleoclimate proxies in the EEP.

2. Study Site and Methods

2.1. Study Site Climatology

The Galápagos Islands (1.5°S to 1.5°N, 92° to 89°W) lie 1,000 km west of the coast of South America (Figure 1). Regional oceanic upwelling and large-scale atmospheric subsidence, due to the descending limb of the Walker Circulation Cell over the EEP, combine to produce the relatively cool and dry climate of the Galápagos. Seasonally, the Galápagos lowlands (sea level to 150 m) experience a warm, rainy season from January to May, which produces 71% of the annual lowland rainfall. In June, a cool, dry season begins as the southeasterly trade winds strengthen, upwelling is enhanced off the coast of South America, and regional SST decreases (Trueman & D'Ozouville, 2010). The subsequent "dry" season in the lowlands lasts through December. At this time, the majority of rain events are coastal drizzle derived from the marine boundary layer stratus clouds (garúa). Cold surface temperatures and an inversion layer created by cooler SST limits convection in the lowlands during the dry season, although this inversion is penetrated by the highlands (>150 m on the windward side of the islands), which have an overall wetter climate due to more garúa precipitation. While the highlands share the same seasonality as the lowlands in terms of temperature, they receive 57% of their annual rainfall during the cool season and 43% during the warm season, and over 500 mm more rainfall annually than the lowlands (Trueman & D'Ozouville, 2010). The position of the Intertropical Convergence

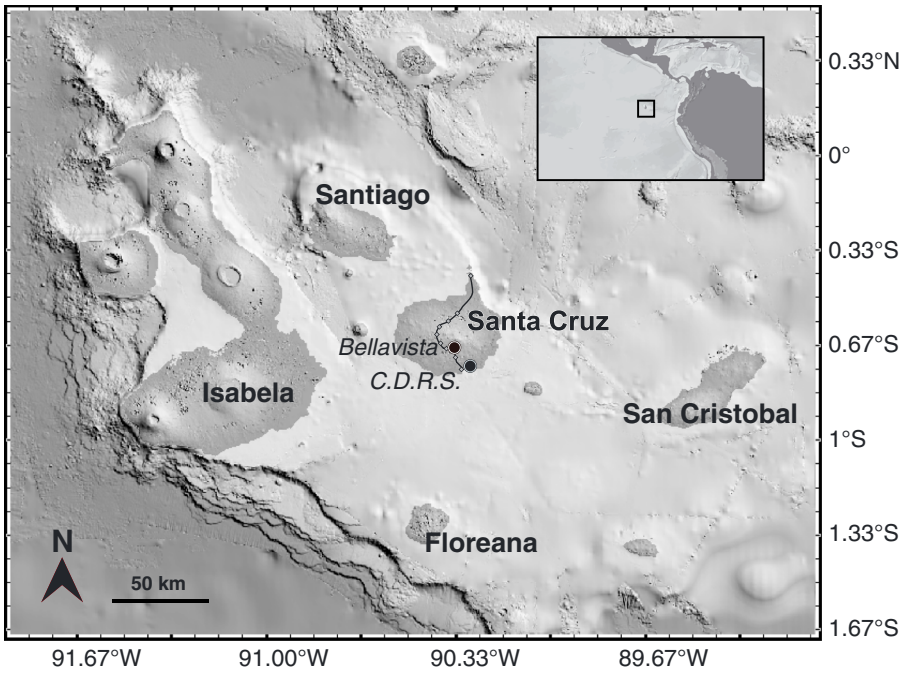

Figure 1. Map of Galápagos, with inset showing location of archipelago relative to South America. Sampling sites on Santa Cruz Island include Charles Darwin Research Station (CDRS, black circle) and Bellavista. Spatial sampling pathway is also drawn on Santa Cruz, with sampling locations represented by diamonds.

Zone (ITCZ) regulates seasonality in the EEP. During the warm season in boreal winter and early spring, the ITCZ is at its southernmost position, decreasing the strength of southeasterly trade winds around the Galápagos (Pisias & Rea, 1988). This leads to a deeper thermocline, warmer SST and increased atmospheric convection in the region (Mitchell & Wallace, 1992). Upon northward migration of the ITCZ in late spring, southeasterly trade winds strengthen, bringing enhanced upwelling, cooler SST and air temperatures, and reduced precipitation to the islands (Colinvaux, 1984).

ENSO is the first-order driver of interannual variability in Galápagos climate. During canonical or Eastern Pacific-type El Niño events that develop off the coast of South America, the southeasterly trade winds weaken, upwelling declines, the thermocline deepens, and the Galápagos experiences warmer than normal SST (Kessler, 2006). Warmer SST leads to deterioration of the atmospheric inversion layer, jumpstarting convection and increasing precipitation in the Galápagos (Trueman & D'Ozouville, 2010). During La Niña events, the Galápagos experiences extremely arid conditions created by anomalously low SST, increased southeasterly trade winds, and increased subsidence (Trueman & D'Ozouville, 2010).

2.2. Sampling Locations and Collection Procedures

A total of 354 event and 14 intraevent precipitation samples were collected from Santa Cruz Island. This island is the second largest of the Galápagos (986 km^2) and lies in the center of the archipelago (0.65°S, 90.35°W), reaching nearly 850 m above sea level at its highest point. Daily precipitation samples were collected at the Charles Darwin Research Station (0°44′37.6″S, 90°50′21.9″W, 2 m above sea level) on the southern coast of the island from 5 October 2012 to 27 March 2016. The Charles Darwin Research Station (CDRS) lies within the arid coastal region of the islands. Precipitation was collected daily, usually at 6:00, using a separatory funnel and mineral oil to guard against evaporation, following IAEA protocols (http://www-naweb.iaea.org), and sampled into 3.5 mL crimp-top vials. During rainier periods, additional samples were collected at 12:00 and 18:00. Amount weighted averages were calculated for days with multiple samples, resulting in 311 daily values. Six samples were excluded from analysis, as they plotted off the local meteoric water line, with negative deuterium excess values 3σ below the mean, suggesting postcollection sample evaporation.

During a January 2015 sampling mission, we collected 19 intraevent precipitation samples at eight sites across the island to assess the island's spatial isotopic variability. The sites lie along the Santa Cruz Highway

Table 1
Site Information for Spatial Precipitation Sampling, 10–18 January 2015

Site	Latitude (°S)	Longitude (°W)	Elevation (m)	Climate zone
0	0.743	90.304	10	Arid
1	0.719	90.326	126	Arid
2	0.694	90.333	200	Transition
3	0.686	90.365	246	Transition
4	0.649	90.405	455	Humid
5	0.641	90.398	539	Humid
6	0.626	90.385	623	Humid
7	0.607	90.367	492	Transition
8	0.490	90.281	21	Arid

Note. No rain was collected at site 8, on the leeward side of Santa Cruz, during the period of collection.

(Figure 1), a major roadway that bisects the island. In total, the range in elevation among our sampling sites was 613 m, with the lowest site near sea level. Of the eight sampling locations along the north/south transect, two were in the arid lowlands, three were in the transition zone (one on the leeward side), and three were in the humid highlands (Table 1). Each day, water from precipitation collectors, consisting of a 14.5 cm diameter funnel, graduated cylinder, and ping pong ball to reduce potential evaporation, was collected, measured, and promptly sealed into 3.5 mL crimp-top vials. Samples with sufficient volume were taken in duplicate.

2.3. Precipitation Measurements

Samples from 2012 to 2016 were measured for $\delta^{18}O$ and δD at the University of Illinois Urbana-Champaign using a Picarro L2130-i cavity ringdown isotopic analyzer. Calibration of the measurements used NIST-VSMOW, NIST-SLAP, and NIST-GISP, with three additional internal standards ($\delta^{18}O$: 0.26‰, −6.81‰, and −10.15‰; δD: 0.6‰, −41.7‰, and −72.3‰) to correct for drift as outlined in van Geldern and Barth (2012). Memory effects between injections of samples during analysis were corrected using empirically derived memory coefficients. No memory effect between samples is attributed to the sampling apparatus because funnel and collector had ample time to dry completely between rain events and collection. Lab experiments recreating field conditions suggest a slight memory effect, less than instrumental precision, may be present in samples collected at the same location in 1 day during our spatial sampling mission due to incomplete drying of collector between sampling times (Conroy et al., 2016). The average standard deviation for duplicate $\delta^{18}O$ measurements of the same sample is 0.04‰ and 0.3‰ for δD. Total instrument uncertainty is $<$0.1‰ for $\delta^{18}O$ and $<$1.0‰ for δD. Individual samples yielding standard deviations of $>$0.1‰ and $>$1.0‰ for $\delta^{18}O$ and δD, respectively, were discarded. To assess monthly values in the data set, the daily 2012–2016 samples were converted to amount-weighted monthly averages. No precipitation occurred in April 2013, so a total of 41 monthly values are assessed.

2.4. Climate and GNIP Isotopic Data

Monthly precipitation isotope data from the Galápagos spanning 1995–2008 (N = 140) were obtained from the International Atomic Energy Agency's GNIP database (IAEA/WMO, 2016; http://www.iaea.org/water). The GNIP station operated continuously in Bellavista (0.71°S, 90.3 W), a small village 180 m above sea level. Bellavista lies within the transition zone between the arid lowland and humid highland climates, with a median annual rainfall of 813 mm. Three GNIP values (October 1999, August 2005, and December 2005) were excluded as they fell substantially below the local meteoric water line, with negative deuterium excess values 3σ below the mean, suggesting postcollection evaporation.

We assess the relationship between $\delta^{18}O_p$ and both regional and local climate data (Figures 2 and S3 in the supporting information). For "regional" data we use spatially averaged SST, precipitation, and outgoing longwave radiation (OLR) within the NIÑO1+2 area (0°–10°S, 90°–80°W). We selected NIÑO1+2 as the ENSO index for assessment based on the strong relationship between Galápagos ocean and climate variables and NIÑO1+2 SST (Conroy et al., 2008). Galápagos SST anomalies over the period of investigation are most strongly correlated with NIÑO1+2 SST relative to NIÑO3, NIÑO3.4, and NIÑO4 SST, as these regions are located much farther west of the extreme eastern equatorial Pacific, the location of the Galápagos (Figure S1). Regional daily and monthly SST and precipitation data used are the Climate Prediction Center Optimally Interpolated SST v2 (Reynolds et al., 2007), Global Precipitation Climatology Project (GPCP) 2.3 monthly precipitation (Adler et al., 2003), and CMOPRH 1.0 global precipitation (Joyce et al., 2004), accessed via Koninklijk Nederlands Meteorologisch Instituut (KNMI) Climate Explorer (Trouet & Van Oldenborgh, 2013). We use NOAA interpolated daily and monthly OLR values for the period prior to January 2014 (Liebmann & Smith, 1996), and NOAA uninterpolated daily OLR values, averaged to monthly resolution, following the cessation of NOAA's interpolated product, provided online by the NOAA/OAR/ESRL PSD, Boulder, Colorado, USA. Local climate data are derived from the weather stations where isotopic data were collected. Monthly and daily weather station data were acquired from the Charles Darwin Research Foundation weather data archive (http://www.darwinfoundation.org/datazone/climate/) for Bellavista and

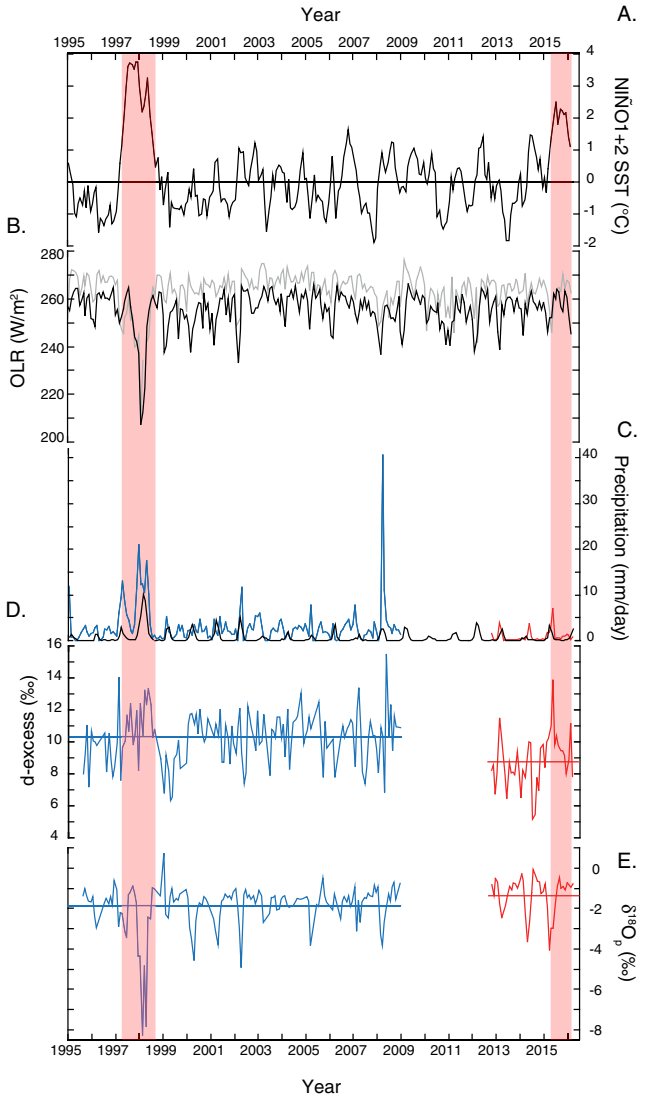

Figure 2. Monthly time series of (a) NIÑO1+2 SST index (°C) (b) OLR (W/m^2) for the 2.5° × 2.5° grid encompassing the Galápagos (gray) and the NIÑO1+2 region (black). Data are derived from uninterpolated NOAA OLR after December 2013. (c) Local precipitation (colored, mm/d) and GPCP2.3 precipitation averaged over the NIÑO1+2 region (black, mm/d). (d) Precipitation d-excess values (‰ VSMOW) and (e) $\delta^{18}O_p$ values (‰ VSMOW). In Figures 2a, 2d, and 2e, long-term means are horizontal lines. Blue color in Figures 2c–2e indicates Bellavista data, red indicates CDRS data. Red shading indicates 1997–1998 and 2015–2016 El Niño events.

Puerto Ayora, Santa Cruz Island, for the time period overlapping the isotope data. We use these data to assess relationships between local climate and the isotopic composition of precipitation. Station variables assessed are air temperature, precipitation amount, and relative humidity.

Backward atmospheric moisture trajectories from 36 days that produced precipitation at CDRS were modeled using the NOAA Air Resource Laboratory Hybrid Single-Particle Lagrangian Integrated Trajectory trajectory model using Global Data Assimilation System 0.5° meteorology (Stein et al., 2015). Three events from each month, consisting of the events with the median, maximum, and minimum daily $\delta^{18}O_p$ values over the period of measurement, were selected for analysis. The coordinates 0.73°S, 90.3°W served as the starting point for each 72 h back trajectory. Initial altitudes of 500 m and 2,000 m were used to capture the movement of air below and above the boundary layer en route to the Galápagos Islands.

3. Results

3.1. Daily Rainfall $\delta^{18}O_p$, δD_p, and D-Excess

Daily $\delta^{18}O_p$ values ranged from −4.5 to 1.1‰, averaging −1.1 ± 0.9‰ (1σ, N = 311). The average daily δD_p value was −0.4 ± 6.4‰ (1σ, N = 311) and ranged from −26.9 to 18.2% over the period of measurement. Daily rainfall deuterium excess (d-excess) had a mean value of 8.4 ± 2.6‰ (1σ, N = 311), ranging from −0.3‰ to 15.6‰. The meteoric water line (MWL), which describes the line of best fit through the daily-resolved $\delta^{18}O_p$ and δD_p values, is defined by $\delta D_p = 6.3 \pm 0.2 \times \delta^{18}O_p + 6.6 \pm 0.4$, 2$\sigma$ (Figure 4).

3.2. Monthly Averaged $\delta^{18}O_p$ and δD_p

Monthly GNIP $\delta^{18}O_p$ values from Bellavista range from −8.20‰ to 0.74‰ (δD_p from −55.7‰ to 12.7‰), with a mean of −1.91 ± 1.15‰, 1σ (δD_p = −5.0 ± 8.9‰, 1σ). Mean d-excess was 10.3‰ ± 1.6‰ (1σ) and ranged from 6.3‰ to 15.5‰. The Bellavista MWL is defined by $\delta D_p = 7.6 \pm 0.2 \times \delta^{18}O_p + 9.6 \pm 0.5$‰, 2$\sigma$ (Figure 4). From February through April, during the height of the wet season, Bellavista precipitation had lower $\delta^{18}O_p$ values, although the standard deviation was also greater in these months (Figure 3a). $\delta^{18}O_p$ was higher in the relatively drier months from May to January. December 1997 to June 1998 exhibited the lowest continuous period of $\delta^{18}O_p$ values (average $\delta^{18}O_p$ = −4.94 ± 2.32‰, 1σ) coinciding with the strong 1997–1998 El Niño event (Figure 2). D-excess during this same time period averaged 11.8 ± 1.8‰ (1σ).

The 2012–2016 data set of amount-weighted monthly $\delta^{18}O_p$ from CDRS ranged from −4.1‰ to −0.1‰ (δD_p from −22.5‰ to 5.7‰), with a mean value of −1.3 ± 0.9‰ (δD_p = −1.7 ± 6.5‰, 1σ). Mean d-excess was 8.8 ± 1.7‰ (1σ) and ranged from 5.2‰ to 13.4‰. The monthly MWL at CDRS is $\delta D_p = 7.0 \pm 0.5 \times \delta^{18}O_p + 7.5 \pm 0.8$, 2$\sigma$ (Figure 4). Monthly averaged data from CDRS show a seasonal cycle, with lower $\delta^{18}O_p$ from March through May, and higher $\delta^{18}O_p$ from June to February (Figure 3b). The period of low $\delta^{18}O_p$ at CDRS extends later in the warm/wet season, into May, relative to the Bellavista data. The 2015/2016 El Niño event is not defined by large deviations in precipitation amount or $\delta^{18}O_p$ relative to the 1997/1998 event, although the lowest observed mean monthly $\delta^{18}O_p$ value at CDRS did occur during the 2015 wet season, at the beginning of the event in March 2015 (−2.9–4.1‰).

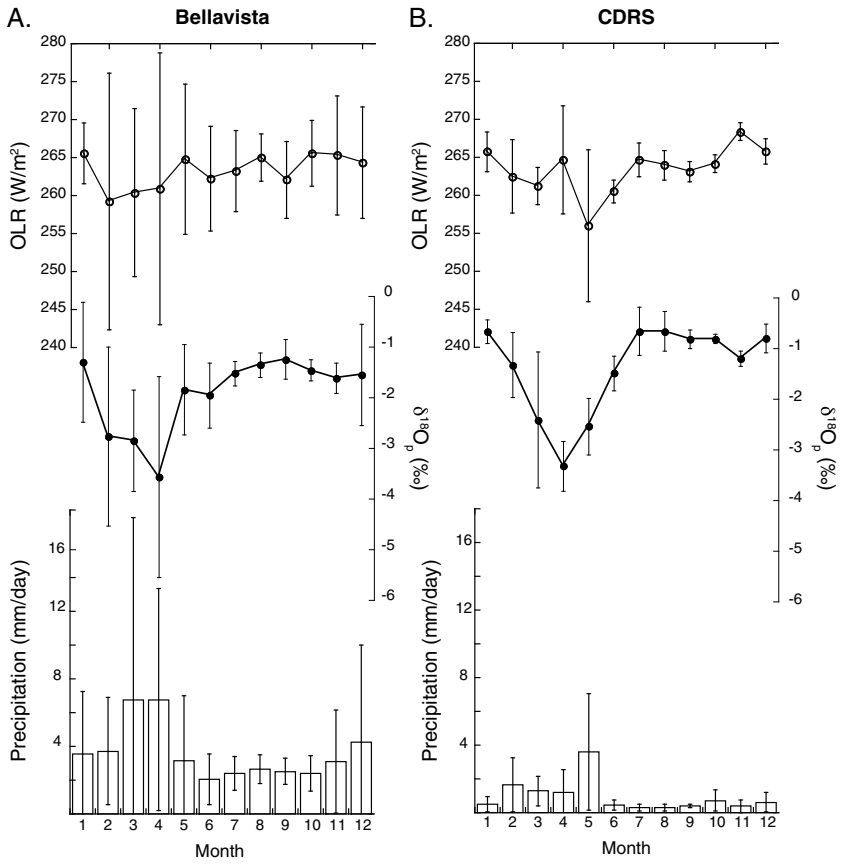

Figure 3. (a) Bellavista (1995–2008) and (b) Charles Darwin Research Station (2012–2016) monthly climatologies of Galápagos OLR (top), $\delta^{18}O_p$ (middle), and precipitation amount (bottom). Error bars represent ±1 standard deviation from the mean. Only OLR and precipitation in months with isotope data are assessed here.

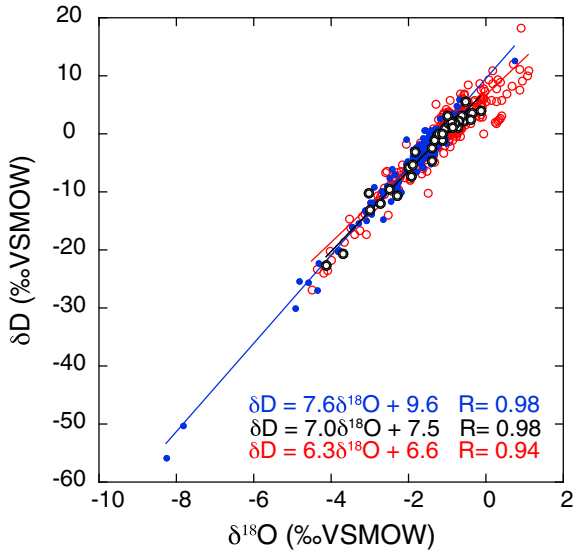

Figure 4. CDRS and Bellavista $\delta^{18}O_p$ and δD_p. Red open circles denote daily CDRS data, black circles denote monthly values from CDRS, and blue circles denote monthly Bellavista data. MWL equations are provided (see text for 2σ values on slopes and intercepts).

3.3. Spatial Variability in $\delta^{18}O_p$ and D-Excess

Precipitation sampled at altitudes ranging from 10 m to 623 m from 10 to 18 January 2015 (Figure 5) shows a significant negative relationship between altitude and $\delta^{18}O_p$ ($R = -0.85$, $N = 19$, $p < 0.001$). Values of $\delta^{18}O_p$ ranged from a low of −1.5‰ in the highlands to a high of 0.1‰ near sea level during this 9 day period. D-excess ranged from 5.0‰ to 10.5‰. A linear regression indicates a −0.2 ± 0.03‰ (1σ) change in $\delta^{18}O_p$ for every 100 m of elevation gain, while d-excess increased 0.5 ± 0.1‰ (1σ) per 100 m altitude gain (R = 0.70, N = 19, $p < 0.001$).

3.4. Air Mass Trajectory Analysis

Boundary layer air masses coincident with measurable precipitation at CDRS predominantly originate from the southeast while air masses from above the mixed layer, or free atmosphere, come primarily from the northeast (Figure 6). There is no clear relationship between rain events with high or low $\delta^{18}O_p$ and moisture trajectory direction. There is also no clear seasonal change in moisture source trajectories, with both the warm/wet season (blue lines in Figure 6) and the cool/dry season (red lines in Figure 6) showing similar moisture pathways. Only 1 month during the warm/wet season, March, shows different trajectories, with air masses coincident with precipitation arriving from the east and west (cyan lines in Figure 6).

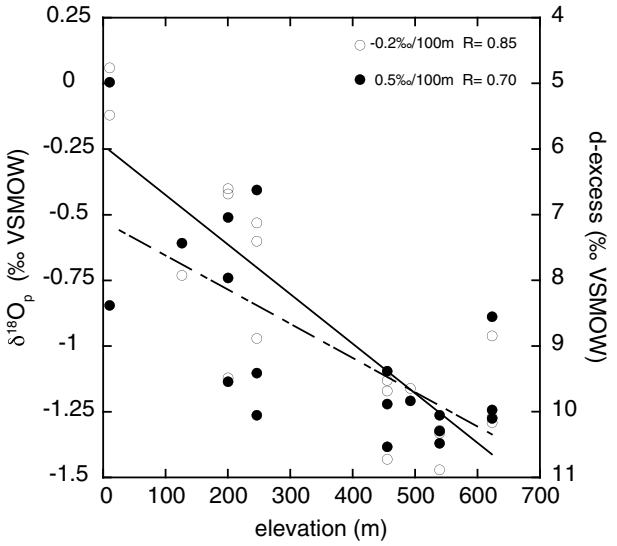

Figure 5. Event-scale 10–18 January 2015 $\delta^{18}O_p$ (open circle) and d-excess (filled circle) values on Santa Cruz Island from samples collected over a range of altitudes. Sampling locations are illustrated in Figure 1.

4. Discussion

4.1. Amount Effect

How the amount effect is manifested throughout the tropical Pacific basin has implications for its underlying mechanisms. Here we analyze the strength of the relationship between both regional and local precipitation amount and Galápagos $\delta^{18}O_p$ to determine the capacity of Galápagos $\delta^{18}O_p$ to record local (station) and regional (i.e., EEP, assessed as the NIÑO1+2 region) precipitation rates. Such spatial differences in the strength of the amount effect are important to consider as they influence the stationarity of $\delta^{18}O_p$-climate relationships over space and time. To that end, inspection of the amount effect at different temporal scales (daily, monthly, seasonal, and interannual) yields useful information about the spectrum of climate processes contained within time-averaged, isotope-based paleoclimate proxies (Moerman et al., 2013).

A similar exercise in northern Borneo (western equatorial Pacific (WEP); 4°N, 115°E) demonstrated that the relationship between local precipitation amount and $\delta^{18}O_p$ was more robust at the monthly time scale ($R = -0.56$, $p < 0.01$) than at the daily time scale ($R = -0.19$, $p < 0.05$) (Moerman et al., 2013). Stronger correlations between regional precipitation and site $\delta^{18}O_p$ versus regional precipitation and local (site) precipitation were also observed in northern Borneo (Moerman et al., 2013). These observations and additional data from other islands and cruises suggest that the WEP amount effect is a product of regional, rather than local atmospheric processes (Kurita, 2013; Kurita et al., 2009). Large-scale climate phenomena like ENSO and the Madden-Julian Oscillation drive the amount effect in the WEP as increases in moisture convergence, convection, and regional precipitation associated with these phenomena can all cause $\delta^{18}O_p$ to decrease downstream.

We find the strength of the amount effect also varies temporally and spatially in the Galápagos. When assessed using the Pearson product moment correlation coefficient (R), local Galápagos precipitation and $\delta^{18}O_p$ show significant, similar negative correlations on both monthly and daily time scales (Table 2). However, the relationship between regional (NIÑO1+2) precipitation and $\delta^{18}O_p$ is higher for monthly Bellavista and monthly CDRS $\delta^{18}O_p$ than for daily CDRS $\delta^{18}O_p$ (Table 2). This result is similar to the time-transgressive nature of the amount effect in Borneo, where the amount effect was also stronger at monthly versus daily time scales.

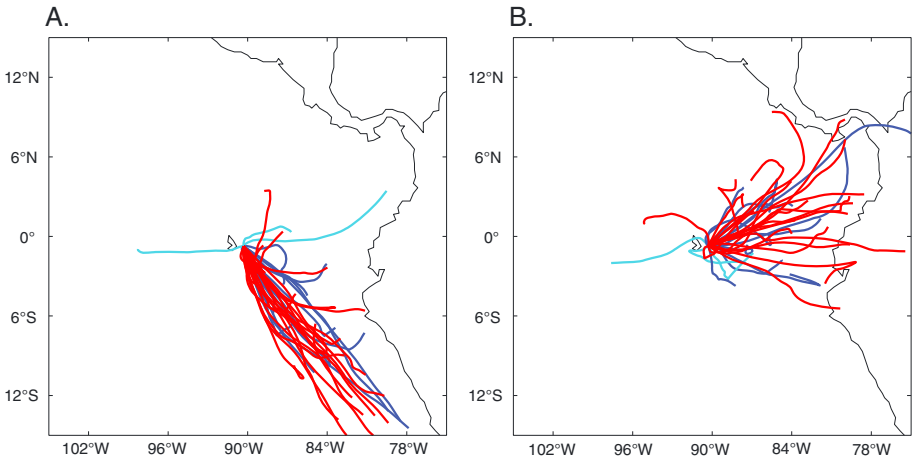

Figure 6. Moisture trajectories within (a) the boundary layer (500 m) and (b) the free troposphere (2,000 m) for precipitation events corresponding to rain events with minimum, maximum, and median $\delta^{18}O_p$ values in each month from 2012 to 2016. Red trajectories denote cool season events from June to December, and blue trajectories denote warm season events from January to May (excluding March). Cyan trajectories indicate events in month of March.

Table 2
Assessment of the Strength of the "Amount Effect:" Pearson Correlation (R) and Spearman's Rank Correlation (ρ) Coefficients Between $\delta^{18}O_p$, Local (Bellavista and Puerto Ayora Weather Stations), and Regional (NIÑO1+2 Area, 0–10°S, 80–90°W) Precipitation and OLR

	NIÑO1+2 precipitation		Local precipitation		NIÑO1+2 OLR		Local OLR	
	R	*ρ*	*R*	ρ	*R*	*ρ*	*R*	*ρ*
Bellavista Monthly	**−0.78**	**−0.42**	**−0.55**	**−0.37**	**0.70**	**0.39**	**0.68**	**0.28**
CDRS Monthly	**−0.50**	−0.32	**−0.57**	**−0.45**	**0.51**	**0.48**	**0.42**	0.22
CDRS Daily	**−0.31**	**−0.38**	**−0.51**	**−0.45**	**0.29**	**0.27**	**0.39**	**0.31**

Note. "Local" OLR is represented by the values from the 2.5° × 2.5° grid containing Santa Cruz. Bold values are significant at 95% confidence level accounting for autocorrelation via effective sample size (Dawdy & Matalas, 1964).

Although the amount effect is often assessed using the Pearson product moment correlation coefficient (*R*), as discussed above (e.g., Cobb et al., 2007; Conroy et al., 2013; Lachniet & Patterson, 2006; Moerman et al., 2013; Rozanski et al., 1993), the Galápagos Islands are a relatively arid location, and the precipitation distribution is skewed by rare, large precipitation events (Figure S2). The distribution of monthly and daily precipitation stable isotope data are also nonnormal (Table S1). Thus, assessment of the relationship between $\delta^{18}O_p$ and precipitation requires the nonparametric Spearman Rank correlation coefficient (ρ), which mitigates the impact of outliers. Spearman's ρ values are presented in comparison to *R* values for precipitation amount versus $\delta^{18}O_p$ in Table 2. Precipitation and $\delta^{18}O_p$ ρ values remain statistically significant but are lower than *R* values, showing a weaker amount affect. For example, monthly regional precipitation and $\delta^{18}O_p$ at Bellavista are highly correlated using Pearson's *R* ($R = -0.78$, $p < 0.001$, $N = 140$). Assessment with Spearman's ρ reduces the strength of the monthly amount effect ($\rho = -0.42$, $p < 0.01$, $N = 140$). With Spearman's ρ, the amount effect is similar at both sites, on monthly and daily time scales, and for local and regional precipitation time series. Given that we do not observe a scaling of amount effect strength with increasing time period (day to month), we cannot make a strong case for the amount effect as only a manifestation of large-scale, time-integrated atmospheric processes, as in the WEP. Rather, the drivers of the daily amount effect observed Galápagos precipitation may be partly related to mechanisms at work during individual storms, such as rainout or increased rain evaporation and exchange with boundary layer vapor at lower rain rates (Dansgaard, 1964).

Correlation maps of Galápagos $\delta^{18}O_p$ and precipitation across the tropical Pacific show that the daily CDRS $\delta^{18}O_p$ has a smaller region of weaker negative correlations closer to (and mainly to the south of) the Galápagos relative to monthly correlation maps (Figure 7a), suggesting the daily-resolution amount effect is driven by more local processes. However, a broader region of stronger correlation coefficients along the equatorial cold tongue region occurs when monthly $\delta^{18}O_p$ from both CDRS and Bellavista are correlated with monthly precipitation (Figures 7b and 7c). This pattern attests to the ability of monthly Galápagos $\delta^{18}O_p$ to represent large-scale atmospheric processes, such as the Walker Circulation. The band of positive correlations to the north of the equator also suggests that ITCZ migration is linked to seasonal isotopic variability in the Galápagos, although the ITCZ does not pass over the site. When the seasonal cycle is removed from the longer Bellavista data set, the observed correlation pattern is more evocative of ENSO, with a region of negative correlations in the cold tongue region and positive correlations in the WEP warm pool (Conroy et al., 2013, Figure 13).

4.2. OLR Versus $\delta^{18}O_p$

Lower OLR values, indicating increased cloud cover, occur during periods of intense convection in the EEP, as seen during the 1997–98 El Niño event (Figure 2). In the western Pacific, one study found a stronger relationship between $\delta^{18}O_p$ and OLR as compared to $\delta^{18}O_p$ versus precipitation (Permana et al., 2016). This relationship may indicate that lower $\delta^{18}O_p$ values record integrative convection rather than local precipitation rates, partly due to the higher cloud top heights and thus colder condensation temperatures that occur during periods of low OLR values (Permana et al., 2016, Scholl et al., 2009). In the Galápagos, we also find significant, positive correlations between OLR and $\delta^{18}O_p$ at daily and monthly time scales. However, using Spearman's ρ, we do not observe a stronger relationship between OLR and $\delta^{18}O_p$ compared to precipitation and $\delta^{18}O_p$, with the exception of monthly CDRS $\delta^{18}O_p$ versus NIÑO1+2 OLR. OLR in the EEP does not solely reflect convective clouds, as the low-lying stratus clouds that produce little precipitation at sea level also coincide with lower

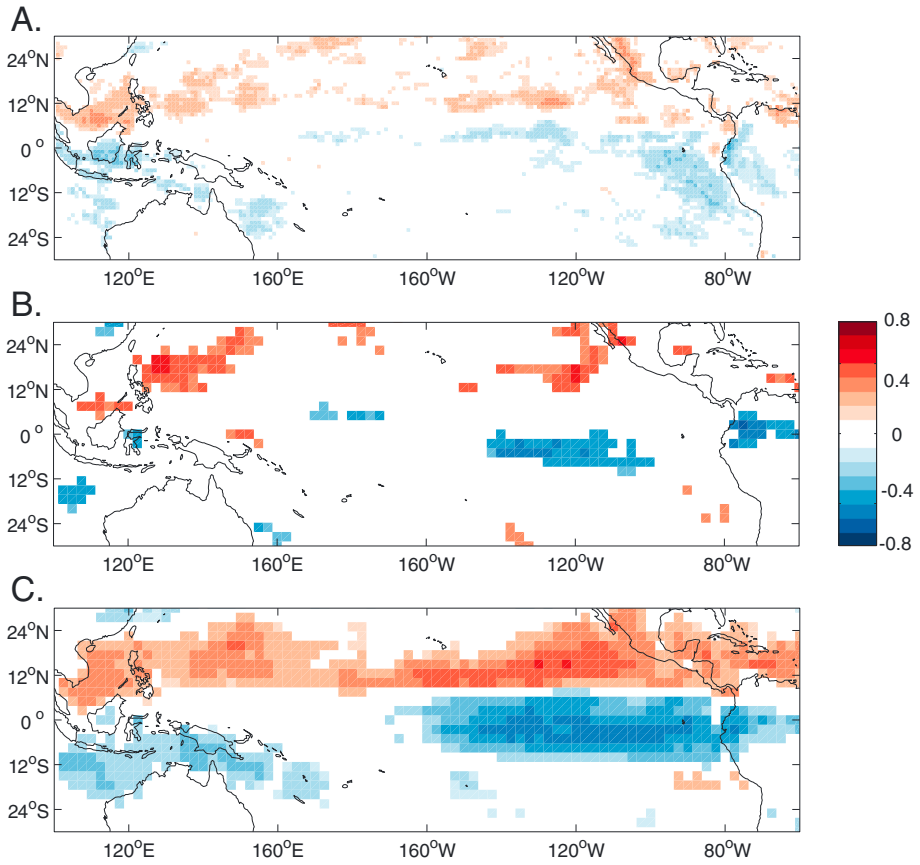

Figure 7. Correlation maps (Spearman rank) of (a) daily Galápagos $\delta^{18}O_p$ from CDRS and daily CMORPH1.0 (CPC MORPHing technique) precipitation, (b) monthly Galápagos $\delta^{18}O_p$ from CDRS and GPCP2.3 precipitation, (c) monthly Galápagos $\delta^{18}O_p$ from Bellavista and GPCP2.3 precipitation. Only correlation coefficients significant at the 95% confidence interval, after accounting for effective sample size, are plotted.

OLR values. Indeed, as observed in Figure 3, there is a weaker seasonality in OLR compared to precipitation and $\delta^{18}O_p$, which may be due to the low OLR values coincident with cool-season stratus clouds as well as warm season convective clouds.

4.3. Elevation Influences on Isotope Values

Monthly $\delta^{18}O_p$ and δD_p values from the higher-elevation Bellavista site and the near sea level CDRS site overlap (Figure 4), and the slopes of the local meteoric water lines defined by monthly averaged isotope data from both sampling locations appear similar (7.6 versus 7.0). However, the two slopes are statistically different ($t = 2.68$, $p < 0.01$, DF = 177). The Bellavista data set contains several months of lower isotope values from the very strong 1997/1998 El Niño event. These low values are likely due to convective processes that have been found to produce lower isotope values in WEP precipitation. However, removing the 10 lowest values, the slope of the MWL is similar ($\delta D_p = 7.1 \pm 0.4 \times \delta^{18}O_p + 8.8 \pm 0.7$, 2σ). The majority of the rain events recorded at CDRS are marine boundary layer drizzle (garúa) or light rain, with precipitation rates <1 mm/d or between 1–10 mm/d, respectively (Figure 8). Garúa and light rain also occur in the highlands, so we hypothesize that differing evaporation rates of falling raindrops in the two different climate zones—the arid lowlands and humid highlands—explain the two distinct MWL slopes. A decrease in MWL slope of an increasingly evaporated body of water (in this case falling raindrops) has been demonstrated empirically (Friedman et al., 1962; Gat, 1996; Gonfiantini, 1986; Stewart, 1975). Therefore, the lower slope at CDRS may be a product of subcloud rainfall evaporation, given the higher aridity in the boundary layer through which precipitation must fall in the lowlands (Friedman et al., 1962; Gat, 1996; Jouzel, 1986).

D-excess values are lower at CDRS relative to Bellavista in both the local MWLs and temporally (Figures 2 and 4). D-excess values are often interpreted in the context of moisture source humidity, temperature, and

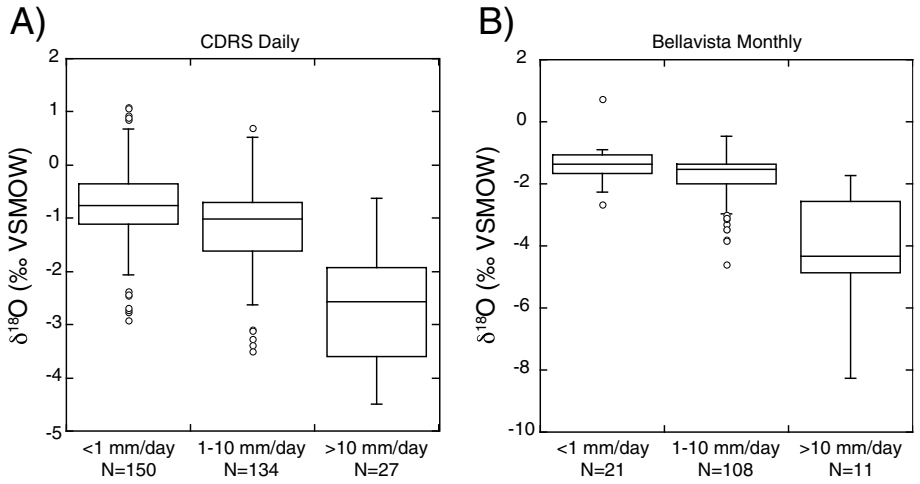

Figure 8. Box and whisker plot showing $\delta^{18}O_p$ values for (a) daily CDRS precipitation samples and (b) monthly Bellavista precipitation samples classified by precipitation rates: <1 mm/d (drizzle), 1–10 mm/d (light rain), and >10 mm/d.

wind speed as these variables drive evaporation and isotopic fractionation (Benetti et al., 2014; Lewis et al., 2013; Masson-Delmotte et al., 2005; Merlivat & Jouzel, 1979; Pfahl & Sodemann, 2014). However, d-excess values in precipitation may also be controlled by conditions or processes during condensation (Risi et al., 2013), with lower d-excess values in precipitation occurring with increased rain evaporation (Conroy et al., 2016). Thus, the lower d-excess values at CDRS relative to Bellavista also support a role for rain evaporation in determining the different stable isotopic composition of precipitation at the two sites.

A 0.2 ± 0.03‰ decrease in $\delta^{18}O_p$ every 100 m in elevation is observed across Santa Cruz (Figure 5) and is comparable to a gradient (~0.21‰/100 m) observed in the Ecuadorian Andes (Poage & Chamberlain, 2001). There is also an increase in d-excess with elevation (Figure 5). The elevation-$\delta^{18}O_p$ and elevation d-excess relationships may be due to two processes: progressive condensation from low to high elevations, associated with island orography, leading to lower $\delta^{18}O_p$ at higher altitudes (i.e., the altitude effect), as well as the previously discussed decrease in rain evaporation in the humid highlands. Spatially, there is not a significant relationship between air temperature and $\delta^{18}O_p$ ($R = 0.35$, $N = 19$, $p = 0.14$). Although we only have near surface temperature measurements from the time of collection, the lack of a spatial temperature-$\delta^{18}O_p$ relationship, despite the strong elevation-$\delta^{18}O_p$ relationship, suggests decreasing condensation temperature with elevation is not producing lower $\delta^{18}O_p$ in this data set. Rather, in the humid highlands, increased relative humidity, frequent garúa and cloud cover, and a shorter distance from cloud to ground may reduce evaporation of falling rain, leading to lower $\delta^{18}O_p$ and higher d-excess values.

The significant difference in slope of the MWL at Bellavista and CDRS and the presence of $\delta^{18}O_p$ and d-excess elevation gradients in precipitation demonstrates the spatial variability in the stable isotopic composition in precipitation on the island, which is less than 1,000 km^2 in total area and only reaches a maximum elevation of 850 m. These findings emphasize the necessity for understanding local meteorological and geographic influences on the isotopic composition of precipitation. Processes such as altitude-dependent rainout of heavy isotopes and differential evaporation rates affecting falling rain may differ significantly over relatively small distances; this is important to consider if isotope-based proxy records from multiple locations are compared.

4.4. Seasonal Variation in Isotope Values

Seasonal changes in moisture source regions in the tropics due to the movement of the ITCZ and related directional shifts in the trade winds can be manifested in $\delta^{18}O_p$. In Borneo, a seasonal $\delta^{18}O_p$ shift of 6‰ is a result of changes in the distance traveled by moisture parcels, and a varying orographic effect dependent on prevailing wind direction, which changes seasonally (Cobb et al., 2007). The long-term seasonal $\delta^{18}O_p$ variability at Bellavista and CDRS is ~2‰ (Figure 3), with lower $\delta^{18}O_p$ occurring in the height of warm/wet season, from February to April in the Bellavista data set and from March to May in the CDRS data set, when precipitation rates are highest. Assessment of atmospheric trajectories leading to precipitation events in the

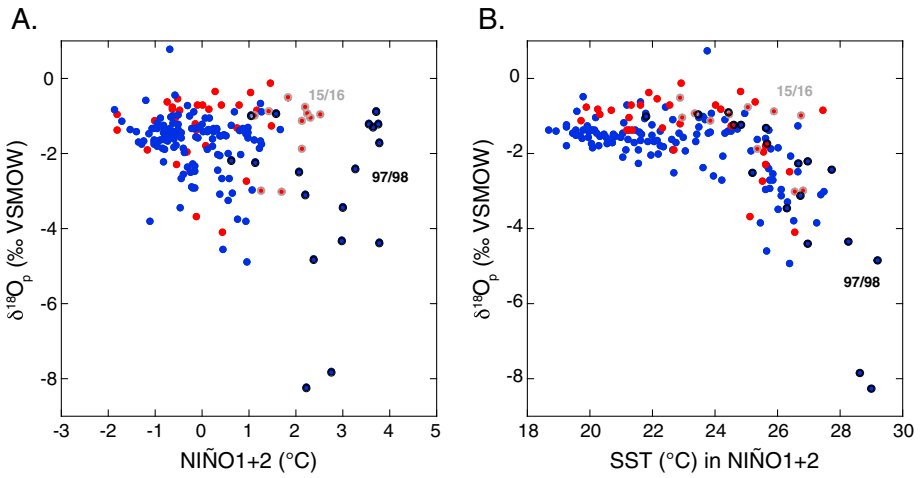

Figure 9. Scatterplot showing (a) NIÑO1+2 SST (°C) and $\delta^{18}O_p$ and (b) SST in NIÑO1+2 region (°C, not anomalies) and $\delta^{18}O_p$. Blue circles indicate Bellavista monthly $\delta^{18}O_p$, and red circles indicate CDRS monthly $\delta^{18}O_p$. Black circle outlines represent monthly $\delta^{18}O_p$ at Bellavista during the 1997–1998 El Niño event (NIÑO1+2 $>$ 0.5°C). Gray circle outlines represent monthly $\delta^{18}O_p$ at CDRS during the 2015–2016 El Niño event (NIÑO1+2 $>$ 0.5°C).

Galápagos Islands from 2012 to 2016 fails to substantiate a clear seasonal relationship between $\delta^{18}O_p$ and moisture source region on seasonal time scales or based on high or low $\delta^{18}O_p$ (Figure 6). Air mass trajectories are consistently from the southeast in the boundary layer and from the northeast above the boundary layer in both the warm/wet and cool/dry seasons. Only 1 month, March (cyan colored lines in Figure 6), has different air mass trajectories, with air parcels arriving from the east and west. March falls within the peak of the warm/wet season, when winds are typically weak, and on average more easterly, near the surface (Trueman & D'Ouzeville, 2010).

Although lower $\delta^{18}O_p$ values in March may be partly attributable to different source regions, overall we hypothesize that seasonal changes in the magnitudes and character of precipitation likely control the observed seasonal $\delta^{18}O_p$ shifts. Throughout most of the year in both locations, excluding the peak of the warm season, precipitation rates are low, dominated by garúa and light rain, which are derived from marine stratus clouds (Trueman & D'Ouzeville, 2010). This type of precipitation likely has relatively high $\delta^{18}O_p$ values due to a more local, marine boundary layer source of the vapor, as well as increased rain evaporation and rain exchange with boundary layer vapor due to the lower rain rates (Figure 8). During larger convective precipitation events in the peak of the warm season, $\delta^{18}O_p$ likely decreases due to processes that are hypothesized to lower $\delta^{18}O_p$ in other marine regions with convective precipitation, such as increased moisture convergence, rain evaporation, and moisture recycling (Risi et al., 2008), occurring both locally and upstream (Conroy et al., 2016).

4.5. ENSO Influences on Isotope Values

How $\delta^{18}O_p$ varies during different phases of ENSO is critical information for assessment of how isotope-based proxy records reflect past ENSO variability (Atwood & Sachs, 2014; Sachs et al., 2009; Zhang et al., 2014). Correlation patterns between Galápagos $\delta^{18}O_p$ and tropical Pacific precipitation (Figure 7) demonstrate an association between $\delta^{18}O_p$ variability and large-scale tropical Pacific circulation. However, it is unclear if $\delta^{18}O_p$ values are distinctive during different ENSO periods. A scatterplot of monthly $\delta^{18}O_p$ from both Bellavista and CDRS versus NIÑO1+2 SST (Figure 9a) shows a range of $\delta^{18}O_p$ values across a large range of NIÑO1+2 SST anomalies. Median Galápagos $\delta^{18}O_p$ values calculated within NIÑO1+2 ENSO categories of strong to very strong El Niño events (NIÑO1+2 SST $>$ 1.5°C), weak to moderate El Niño events (NIÑO1+2 SST $<$1.5°C and $>$0.5°C), "neutral" conditions (NIÑO1+2 SST between $-$0.5°C and 0.5°C), weak La Niña events (NIÑO1+2 SST $>$ $-$1°C and $<$ $-$0.5°C), and moderate to strong La Niña events (NIÑO1+2 SST $<$ $-$1°C) show median $\delta^{18}O_p$ varies with ENSO categories in warm season months only (Table S2). From January to May, $\delta^{18}O_p$ is higher during La Niña periods and lower during El Niño periods. In cold season months, median $\delta^{18}O_p$ does not vary with ENSO category (Table S2). The results of a nonparametric Wilcoxan rank-sum test for significant differences between $\delta^{18}O_p$ distributions for these ENSO phase categories also show that

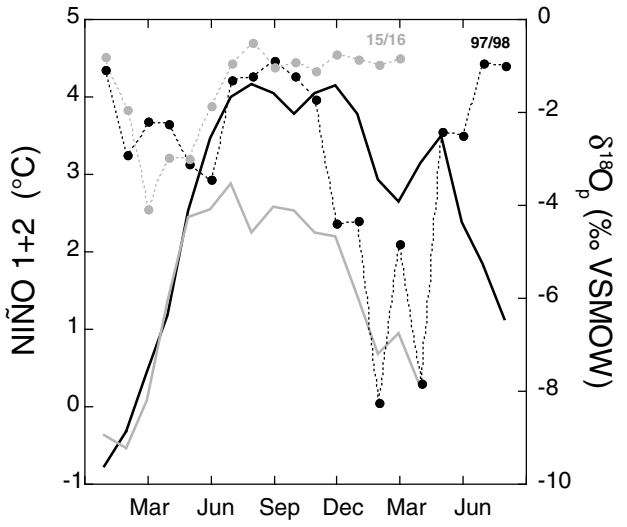

Figure 10. Monthly development of 1997/1998 (black lines) and 2015/2016 (gray lines) El Niño events as recorded by NIÑO1+2 SST anomalies (solid lines) and Galápagos $\delta^{18}O_p$ (dashed lines).

cool season $\delta^{18}O_p$ values are not significantly different in different ENSO categories (Table S3). However, even during the warm season, median $\delta^{18}O_p$ is not significantly different in weak to moderate El Niño periods, neutral, and La Niña periods. Thus, a large portion of the ENSO spectrum may not be identified in the Galápagos based on $\delta^{18}O_p$ values alone.

The magnitude of SST is important in determining whether deep convection can occur (Graham & Barnett, 1987). We find that an SST threshold must be surpassed to produce the lowest $\delta^{18}O_p$ values measured in the Galápagos. Substantially lower $\delta^{18}O_p$ values (<-5‰) occur only when SST is above 28°C (Figure 9b). During the 1997/1998 El Niño event, sustained high SST anomalies extended into the 1998 warm season months, increasing SST above the deep convection threshold and producing abundant rainfall with low $\delta^{18}O_p$ values during this event (Figure 10). The 2015/2016 El Niño event, expressed in the NIÑO1+2 metric, began similarly and is the only El Niño event since 1997/1998 where SST anomalies reached similar, sustained, high levels (Figure 2). Even so, during the 2015/2016 El Niño, SST abruptly cooled in the beginning of the warm season, and no large precipitation events occurred. Thus, the 2015/2016 El Niño, one of the largest El Niños recorded, did not manifest itself in eastern Pacific precipitation or in the stable isotopic composition of Galápagos precipitation.

Precipitation d-excess can provide additional insight into atmospheric processes at work during ENSO events. In a daily-resolved data set from Costa Rica, the 2015/2016 El Niño event was not strongly manifested in $\delta^{18}O_p$ or δD_p values but was associated with decreasing d-excess values in precipitation, attributed to changing moisture flux convergence in this area (Sánchez-Murillo et al., 2016). In the Galápagos, monthly d-excess at CDRS reached its maximum value during the 2015/2016 El Niño (Figure 2). D-excess was also high relative to the long-term mean at Bellavista during the 1997/1998 El Niño (Figure 2). The period of lowest, sustained, monthly d-excess values in the Galápagos occurred from 1999 to 2000, a La Niña period following the strong 1997–1998 El Niño (Figure 2). We also observe significant, positive correlations between Galápagos precipitation and d-excess and monthly and daily time scales (Table S4). However, d-excess correlations with air temperature, relative humidity, NIÑO1+2 SST, and NIÑO1+2 precipitation are weaker, and insignificant for OLR, suggesting that conditions during local condensation modifies precipitation d-excess values in the Galápagos. During cool, dry periods, lower d-excess values may be a result of greater evaporation of rain, whereas higher d-excess values (near or approaching the global mean value of 10) occur during periods with greater precipitation.

4.6. Paleoclimate Implications

Recent efforts to constrain past hydroclimate using proxies for the stable isotopic composition of meteoric waters in the Galápagos focus on an ENSO and ITCZ-driven amount effect signal (Atwood & Sachs, 2014; Nelson and Sachs, 2016; Zhang et al., 2014). One appeal of proxy records of the stable isotopic composition of precipitation, relative to other types of proxies for rainfall intensity and El Niño in the region, is that they should capture a range of variability, including periods of high and low precipitation. In contrast, sedimentological proxies for ENSO-related EEP precipitation often only show variability at the El Niño end of the ENSO spectrum (Conroy et al., 2008; Moy et al., 2002; Riedinger et al., 2002). Figure 7 demonstrates that daily to monthly variability in Galápagos $\delta^{18}O_p$ reflects large-scale tropical Pacific circulation. However, in time-averaged, isotope-based proxy records where monthly variability is not preserved, there may be a bias toward strong El Niño events, similar to the bias in other sediment-based ENSO proxies. That is, since median $\delta^{18}O_p$ in weak to moderate El Niño periods cannot be distinguished from median $\delta^{18}O_p$ in La Niña or neutral periods (Table S3), it may be challenging to identify all but the strongest El Niño events in time-averaged isotope proxy records. Additionally, records from the Galápagos highlands, which can receive substantial precipitation in cool season months, may have a more muted ENSO signal, given that cool-season $\delta^{18}O_p$ does not vary across the ENSO spectrum (Tables S2 and S3). Yet processes affecting the stable isotopic

composition of water other than the stable isotopic composition of precipitation are also important to consider. For example, the balance of precipitation/evaporation and groundwater inputs can amplify or attenuate the precipitation amount signal in lake water $\delta^{18}O/\delta D$. This places an increased importance of hydrologic modeling for studies that interpret isotope-based proxy records of precipitation.

From site to site across the Galápagos, different mechanisms may have greater relative importance in controlling stable isotopic values of precipitation, which may affect how proxy records are interpreted site to site, even across relatively small distances. As revealed by the assessment of MWLs and the altitude effect, evaporation is more important in the arid lowlands versus the humid highlands. More broadly, we do not see clear evidence for the amount effect to be interpreted as a result of shifting moisture source regions or solely as a result of large-scale moisture convergence and organized convection, as observed in the WEP. This is due to the lack of an observed relationship between moisture trajectories and $\delta^{18}O_p$ as well as a strong amount effect manifested on the single-event (daily) time scale. However, moisture convergence and large-scale organized convection likely play a key role in determining $\delta^{18}O_p$ and the amount effect during very strong El Niño events when EEP SST surpasses the deep convection threshold. The significant daily amount effect in the Galapagos highlights the importance of local as well as regional influences on the $\delta^{18}O_p$-precipitation relationship.

5. Conclusions

This study provides the first daily-resolved record of stable isotopes in precipitation from an island site in the EEP, allowing us to investigate the relationship between climate and stable isotopes in precipitation at both daily and monthly time scales. Unlike the WEP, where no significant amount effect is apparent on daily time scales (Moerman et al., 2013), Galápagos data reveal a significant negative correlation between daily as well as monthly precipitation amount and $\delta^{18}O_p$. Accounting for the nonnormal distribution of precipitation in the Galápagos, the strength of the amount effect is similar at monthly and daily time scales. Analysis of meteoric water lines and d-excess from the higher-elevation Bellavista site and the near sea level CDRS site suggests that differences in aridity between the arid lowlands and humid highlands produce distinct isotopic values in precipitation. The strength of the amount effect on daily time scales in the Galápagos may testify to the role of varying rates of rain evaporation, equilibrium with boundary layer vapor, and rainout effects during individual storms in shaping the precipitation-$\delta^{18}O_p$ relationship in the arid EEP. This stands in contrast to the WEP warm pool, where a stronger amount effect at monthly versus daily time scales suggests a greater influence of factors such as moisture convergence and moisture pathways.

In the Galápagos, precipitation characteristics vary with ENSO. The majority of rain events observed isotopically in the Galápagos during La Niña through strong El Niños are locally derived drizzle or light rain, ("garúa"), with corresponding high $\delta^{18}O_p$ values. The significantly lower $\delta^{18}O_p$ during very strong El Niños is a result of warmer warm seasons, when regional SST surpasses the threshold for deep convection. During these periods, convective processes produce low $\delta^{18}O_p$. On monthly time scales, only rare months of high precipitation during very strong El Niño events during the height of the warm season produce extremely negative $\delta^{18}O_p$ values, a bias to consider when interpreting time-averaged stable isotope-based paleoclimate proxies in the region. Although proxy records of $\delta^{18}O_p$ or δD_p hold the potential to capture hydroclimatic variability for this region throughout the Holocene, our findings indicate that stable isotope values of precipitation in the Galápagos can vary across relatively small spatial scales, a result to consider when interpreting stable isotope-based paleoclimate proxy records from multiple highland and lowland locations. Additionally, the inability of $\delta^{18}O_p$ to separate weak to moderate El Niño periods from La Niña and neutral periods in warm season precipitation, as well as the lack of a difference in $\delta^{18}O_p$ distributions across the ENSO spectrum in cool season months, still necessitates the collection of multiple, diverse measurements to stitch together past ENSO variability in the Galápagos.

Acknowledgments
We thank the Charles Darwin Research Station and Galápagos National Park for sample permits and logistical support. Funding sources for this work includes NSF-AGS-PF 1049664 to J. L. C., University of Illinois Urbana-Champaign, Department of Geology to J. L. C., NSF ATM-1203785 to K. M. C. and J. L. C., and NSF ATM-1464824, NNX08AR23G, and 07-NEWS07-0020 to D. N. Stable isotope data are available as supporting information online at http://onlinelibrary.wiley.com/doi/10.1002/201XXXX and have also been archived on the IAEA GNIP database at https://nucleus.iaea.org/wiser.

References

Adler, R. F., Huffman, G. J., Chang, A., Ferraro, R., Xie, P.-P., Janowiak, J., … Bolvin, D. (2003). The version-2 global precipitation climatology project (GPCP) monthly precipitation analysis (1979-present). *Journal of Hydrometeorology*, *4*(6), 1147–1167.

Atwood, A. R., & Sachs, J. P. (2014). Separating ITCZ- and ENSO-related rainfall changes in the Galápagos over the last 3 kyr using D/H ratios of multiple lipid biomarkers. *Earth and Planetary Science Letters*, *404*, 408–419. https://doi.org/10.1016/j.epsl.2014.07.038

Benetti, M., Reverdin, G., Pierre, C., Merlivat, L., Risi, C., Steen-Larsen, H. C., & Vimeux, F. (2014). Deuterium excess in marine water vapor: Dependency on relative humidity and surface wind speed during evaporation. *Journal of Geophysical Research: Atmospheres*, *119*, 584–593. https://doi.org/10.1002/2013JD020535

Berkelhammer, M., Sinha, A., Stott, L., Cheng, H., Pausata, F. S. R., & Yoshimura, K. (2012). An abrupt shift in the Indian monsoon 4000 years ago. In L. Giosan, et al. (Eds.), *Climates, landscapes, civilizations* (pp. 75–88). Washington: American Geophysical Union.

Cai, W. J., Santoso, A., Wang, G. J., Yeh, S. W., An, S. I., Cobb, K. M., … Wu, L. X. (2015). ENSO and greenhouse warming. *Nature Climate Change*, *5*(9), 849–859. https://doi.org/10.1038/nclimate2743

Carré, M., Sachs, J. P., Purca, S., Schauer, A. J., Braconnot, P., Falcón, R. A., … Lavallée, D. (2014). Holocene history of ENSO variance and asymmetry in the eastern tropical Pacific. *Science*, *345*(6200), 1045–1048. https://doi.org/10.1126/science.1252220

Cobb, K. M., Adkins, J. F., Partin, J. W., & Clark, B. (2007). Regional-scale climate influences on temporal variations of rainwater and cave dripwater oxygen isotopes in northern Borneo. *Earth and Planetary Science Letters*, *263*(3-4), 207–220. https://doi.org/10.1016/j.epsl.2007.08.024

Colinvaux, P. A. (1984). The Galapagos climate: Present and past. In R. Perry (Ed.), *Key environments: Galapagos* (pp. 55–69). Oxford: Pergamon Press.

Conroy, J. L., Cobb, K. M., & Noone, D. (2013). Comparison of precipitation isotope variability across the tropical Pacific in observations and SWING2 model simulations. *Journal of Geophysical Research: Atmospheres*, *118*, 5867–5892. https://doi.org/10.1002/jgrd.50412

Conroy, J. L., Noone, D., Cobb, K. M., Moerman, J. W., & Konecky, B. L. (2016). Paired stable isotopologues in precipitation and vapor: A case study of the amount effect within western tropical Pacific storms. *Journal of Geophysical Research: Atmospheres*, *121*, 3290–3303. https://doi.org/10.1002/2015JD023844

Conroy, J. L., Overpeck, J. T., Cole, J. E., Shanahan, T. M., & Steinitz-Kannan, M. (2008). Holocene changes in eastern tropical Pacific climate inferred from a Galápagos lake sediment record. *Quaternary Science Reviews*, *27*(11-12), 1166–1180. https://doi.org/10.1016/j.quascirev.2008.02.015

Conroy, J. L., Restrepo, A., Overpeck, J. T., Steinitz-Kannan, M., Cole, J. E., Bush, M. B., & Colinvaux, P. A. (2009). Unprecedented recent warming of surface temperatures in the eastern tropical Pacific Ocean. *Nature Geoscience*, *2*(1), 46–50. https://doi.org/10.1038/ngeo390

Dansgaard, W. (1964). Stable isotopes in precipitation. *Tellus*, *16*(4), 436–468. https://doi.org/10.1111/j.2153-3490.1964.tb00181.x

Dawdy, D. R., & Matalas, N. C. (1964). Statistical and probability analysis of hydrologic data, part III: Analysis of variance, covariance and time series. In V. T. Chow (Ed.), *Handbook of applied hydrology, a compendium of water-resources technology* (pp. 8.68–68.90). New York: McGraw-Hill Book Company.

Dunbar, R. B., Wellington, G. M., Colgan, M. W., & Glynn, P. W. (1994). Eastern Pacific sea surface temperature since 1600 A.D.: The?18O record of climate variability in Galápagos corals. *Paleoceanography*, *9*(2), 291–315. https://doi.org/10.1029/93PA03501

Friedman, I., Machta, L., & Soller, R. (1962). Water vapor exchange between a water droplet and its environment. *Journal of Geophysical Research*, *67*(7), 2761–2766. https://doi.org/10.1029/JZ067i007p02761

Gat, J. R. (1996). Oxygen and hydrogen isotopes in the hydrologic cycle. *Annual Review of Earth and Planetary Sciences*, *24*(1), 225–262. https://doi.org/10.1146/annurev.earth.24.1.225

Gonfiantini, R. (1986). Environmental isotopes in lake studies. In P. Fritz & J. C. Fontes (Eds.), *Handbook of Environment Isotope geochemistry*, (Vol. 2, pp. 113–168). Amsterdam: Elsevier.

Graham, N. E., & Barnett, T. P. (1987). Sea surface temperature, surface wind divergence, and convection over tropical oceans. *Science*, *238*(4827), 657–659. https://doi.org/10.1126/science.238.4827.657

IAEA (2016). Global Network of Isotopes in Precipitation. The GNIP database. Accessible at: http://www.iaea.org/water

Johnson, N. C. (2013). How many ENSO flavors can we distinguish?*. *Journal of Climate*, *26*(13), 4816–4827. https://doi.org/10.1175/JCLI-D-12-00649.1

Jouzel, J. (1986). Isotopes in cloud physics: Multiphase and multistage condensation processes. In P. Fritz & J. C. Fontes (Eds.), *Handbook of Environmental Isotope Geochemistry* (Vol. 2, pp. 61–112). Amsterdam, Netherlands: Elsevier.

Joyce, R. J., Janowiak, J. E., Arkin, P. A., & Xie, P. (2004). CMORPH: A method that produces. global precipitation estimates from passive microwave and infrared data at high spatial and temporal resolution. *Journal of Hydrometeorology*, *5*(3), 487–503. https://doi.org/10.1175/1525-7541(2004)005%3C0487:CAMTPG%3E2.0.CO;2

Kessler, W. S. (2006). The circulation of the eastern tropical Pacific: A review. *A Review Eastern Tropical Pacific Oceanography*, *69*(2-4), 181–217. https://doi.org/10.1016/j.pocean.2006.03.009

Koutavas, A., & Lynch-Stieglitz, J. (2004). Variability of the marine ITCZ over the eastern Pacific during the past 30,000 years. In *The Hadley circulation: Present, past and future* (pp. 347–369). Dordrecht, Netherlands: Springer. https://doi.org/10.1007/978-1-4020-2944-8_13

Koutavas, A., Lynch-Stieglitz, J., Marchitto, T. M., & Sachs, J. P. (2002). El Nino-like pattern in ice age tropical Pacific sea surface temperature. *Science*, *297*(5579), 226–230. https://doi.org/10.1126/science.1072376

Koutavas, A., Olive, G. C., & Lynch-Stieglitz, J. (2006). Mid-Holocene El Niño–Southern Oscillation (ENSO) attenuation revealed by individual foraminifera in eastern tropical Pacific sediments. *Geology*, *34*(12), 993–996. https://doi.org/10.1130/G22810A.1

Kug, J.-S., Jin, F.-F., & An, S.-I. (2009). Two types of El Niño events: Cold tongue El Niño and warm pool El Niño. *Journal of Climate*, *22*(6), 1499–1515. https://doi.org/10.1175/2008JCLI2624.1

Kurita, N. (2013). Water isotopic variability in response to mesoscale convective system over the tropical ocean. *Journal of Geophysical Research: Atmospheres*, *118*, 10,376–10,390. https://doi.org/10.1002/jgrd.50754

Kurita, N., Ichiyanagi, K., Matsumoto, J., Yamanaka, M. D., & Ohata, T. (2009). The relationship between the isotopic content of precipitation and the precipitation amount in tropical regions. *Isoscapes Isotopes Mapping its Application Isoscapes 2008*, *102*(3), 113–122. https://doi.org/10.1016/j.gexplo.2009.03.002

Lachniet, M. S., & Patterson, W. P. (2006). Use of correlation and stepwise regression to evaluate physical controls on the stable isotope values of Panamanian rain and surface waters. *Journal of Hydrology*, *324*(1-4), 115–140. https://doi.org/10.1016/j.jhydrol.2005.09.018

Lawrence, J. R., Gedzelman, S. D., Dexheimer, D., Cho, H., Carrie, G. D., Gasparini, R., … Biggerstaff, M. I. (2004). Stable isotopic composition of water vapor in the tropics. *Journal of Geophysical Research*, *109*, D06115. https://doi.org/10.1029/2003JD004046

Lea, D. W., Pak, D. K., & Spero, H. J. (2000). Climate impact of late Quaternary equatorial Pacific sea surface temperature variations. *Science*, *289*(5485), 1719–1724. https://doi.org/10.1126/science.289.5485.1719

Lewis, S. C., LeGrande, A. N., Kelley, M., & Schmidt, G. A. (2013). Modeling insights into deuterium excess as an indicator of water vapor source conditions. *Journal of Geophysical Research: Atmospheres*, *118*, 243–262. https://doi.org/10.1029/2012JD017804

Liebmann, B., & Smith, C. A. (1996). Description of a complete (interpolated) outgoing longwave radiation dataset. *Bulletin of the American Meteorological Society*, *77*, 1275–1277.

Loubere, P., Richaud, M., Liu, Z., & Mekik, F. (2003). Oceanic conditions in the eastern equatorial Pacific during the onset of ENSO in the Holocene. *Quaternary Research*, *60*(02), 142–148. https://doi.org/10.1016/S0033-5894(03)00092-9

Masson-Delmotte, V., Jouzel, J., Landais, A., Stievenard, M., Johnsen, S. J., White, J. W. C., … Fuhrer, K. (2005). GRIP deuterium excess reveals rapid and orbital-scale changes in Greenland moisture origin. *Science*, *309*(5731), 118–121. https://doi.org/10.1126/Science.1108575

Merlivat, L., & Jouzel, J. (1979). Global climatic interpretation of the deuterium-oxygen 18 relationship for precipitation. *Journal of Geophysical Research*, *84*(C8), 5029–5033. https://doi.org/10.1029/JC084iC08p05029

Mitchell, T. P., & Wallace, J. M. (1992). The annual cycle in equatorial convection and sea surface temperature. *Journal of Climate*, *5*(10), 1140–1156. https://doi.org/10.1175/1520-0442(1992)005%3C1140:TACIEC%3E2.0.CO;2

Moerman, J. W., Cobb, K. M., Adkins, J. F., Sodemann, H., Clark, B., & Tuen, A. A. (2013). Diurnal to interannual rainfall δ18O variations in northern Borneo driven by regional hydrology. *Earth and Planetary Science Letters*, *369–370*(Supplement C), 108–119. https://doi.org/10.1016/j.epsl.2013.03.014

Moy, C. M., Seltzer, G. O., Rodbell, D. T., & Anderson, D. M. (2002). Variability of El Niño/Southern Oscillation activity at millennial timescales during the Holocene epoch. *Nature*, *420*(6912), 162–165. https://doi.org/10.1038/nature01194

Nelson, D. B., & Sachs, J. P. (2016). Galápagos hydroclimate of the Common Era from paired microalgal and mangrove biomarker 2H/1H values. *Proceedings of the National Academy of Sciences*, *113*(13), 3476–3481. https://doi.org/10.1073/pnas.1516271113

Permana, D. S., Thompson, L. G., & Setyadi, G. (2016). Tropical West Pacific moisture dynamics and climate controls on rainfall isotopic ratios in southern Papua, Indonesia. *Journal of Geophysical Research: Atmospheres*, *121*, 2222–2245. https://doi.org/10.1002/2015JD023893

Pfahl, S., & Sodemann, H. (2014). What controls deuterium excess in global precipitation? *Climate of the Past*, *10*(2), 771–781. https://doi.org/10.5194/cp-10-771-2014

Pisias, N. G., & Rea, D. K. (1988). Late Pleistocene paleoclimatology of the central equatorial Pacific: Sea surface response to the southeast trade winds. *Paleoceanography*, *3*(1), 21–37. https://doi.org/10.1029/PA003i001p00021

Poage, M. A., & Chamberlain, C. P. (2001). Empirical relationships between elevation and the stable isotope composition of precipitation and surface waters: Considerations for studies of paleoelevation change. *American Journal of Science*, *301*(1), 1–15. https://doi.org/10.2475/ajs.301.1.1

Reynolds, R. W., Smith, T. M., Liu, C., Chelton, D. B., Casey, K. S., & Schlax, M. G. (2007). Daily high-resolution-blended analyses for sea surface temperature. *Journal of Climate*, *20*(22), 5473–5496. https://doi.org/10.1175/2007JCLI1824.1

Riedinger, M., Steinitz-Kannan, M., Last, W., & Brenner, M. (2002). A 6100 14C yr record of El Niño activity from the Galapagos Islands. *Journal of Paleolimnology*, *27*(1), 1–7. https://doi.org/10.1023/A:1013514408468

Risi, C., Bony, S., & Vimeux, F. (2008). Influence of convective processes on the isotopic composition d18O and dD of precipitation and water vapor in the tropics: 2. Physical interpretation of the amount effect. *Journal of Geophysical Research*, *113*, D19306. https://doi.org/10.1029/2008JD009943

Risi, C., Landais, A., Winkler, R., & Vimeux, F. (2013). Can we determine what controls the spatio- temporal distribution of d-excess and O-17-excess in precipitation using the LMDZ general circulation model? *Climate of the Past*, *9*(5), 2173–2193. https://doi.org/10.5194/cp-9-2173-2013

Rozanski, K., Araguás-Araguás, L., & Gonfiantini, R. (1993). Isotopic patterns in modern global precipitation. In *Climate Change in Continental Isotopic Records* (pp. 1–36). Washington, DC: American Geophysical Union.

Sachs, J. P., Sachse, D., Smittenberg, R. H., Zhang, Z., Battisti, D. S., & Golubic, S. (2009). Southward movement of the Pacific intertropical convergence zone AD 1400–1850. *Nature Geoscience*, *2*(7), 519–525. https://doi.org/10.1038/ngeo554

Sánchez-Murillo, R., Durán-Quesada, A. M., Birkel, C., Esquivel-Hernández, G., & Boll, J. (2016). Tropical precipitation anomalies and d-excess evolution during El Niño 2014–16. *Hydrological Processes*, *31*(4), 956–967. https://doi.org/10.1002/hyp.11088

Scholl, M. A., Shanley, J. B., Zegarra, J. P., & Coplen, T. B. (2009). The stable isotope amount effect: New insights from NEXRAD echo tops, Luquillo Mountains, Puerto Rico. *Water Resources Research*, *45*, W12407. https://doi.org/10.1029/2008WR007515

Stein, A. F., Draxler, R. R., Rolph, G. D., Stunder, B. J. B., Cohen, M. D., & Ngan, F. (2015). NOAA's HYSPLIT atmospheric transport and dispersion modeling system. *Bulletin of the American Meteorological Society*, *96*(12), 2059–2077. https://doi.org/10.1175/BAMS-D-14-00110.1

Stewart, M. K. (1975). Stable isotope fractionation due to evaporation and isotopic exchange of falling waterdrops: Applications to atmospheric processes and evaporation of lakes. *Journal of Geophysical Research*, *80*(9), 1133–1146. https://doi.org/10.1029/JC080i009p01133

Trouet, V., & Van Oldenborgh, G. J. (2013). KNMI Climate Explorer: A web-based research tool for high-resolution paleoclimatology. *Tree-Ring Research*, *69*(1), 3–13. https://doi.org/10.3959/1536-1098-69.1.3

Trueman, M., & D'Ozouville, N. (2010). Characterizing the Galápagos terrestrial climate in the face of global climate change. *Gal'pagos Research*, *67*, 26–37.

van Geldern, R., & Barth, J. A. C. (2012). Optimization of instrument setup and post-run corrections for oxygen and hydrogen stable isotope measurements of water by isotope ratio infrared spectroscopy (IRIS). *Limnology and Oceanography: Methods*, *10*(12), 1024–1036. https://doi.org/10.4319/lom.2012.10.1024

Yapp, C. J. (1982). A model for the relationships between precipitation D/H ratios and precipitation intensity. *Journal of Geophysical Research*, *87*(C12), 9614–9620. https://doi.org/10.1029/JC087iC12p09614

Zhang, Z., Leduc, G., & Sachs, J. P. (2014). El Nino evolution during the Holocene revealed by a biomarker rain gauge in the Galapagos Islands. *Earth and Planetary Science Letters*, *404*, 420–434. https://doi.org/10.1016/j.epsl.2014.07.013